SLOWKIN: A SIMPLIFIED MODEL FOR THE SIMULATION OF REACTOR TRANSIENTS IN SLOWPOKE-2

D. ROZON AND S. KAVEH

Institut de génie nucléaire, École Polytechnique de Montréal
P.O. Box 6079, Station Centre Ville, Montréal, Québec H3C 3A7 CANADA
E-mail: rozon@meca.polymtl.ca

I. Introduction

This paper will describe the model used to analyse reactor transients in the SLOWPOKE–2 reactor at École Polytechnique. The model is intended to simulate reactor transients which will be induced by control rod displacements during commissionning of the new LEU core to be installed in the SLOWPOKE–2 reactor in 1997, in replacement of the original HEU core.[1] A simplified treatment is justified since our objective is mainly to provide a physical interpretation for any difference observed in the transient behaviour of the new core, as opposed to the current HEU core.

The SLOWKIN model uses point kinetics to predict neutron power with time. The reactor physics codes DRAGON/DONJON were used to provide some reactor physics insight on the strong neutronic/thermalhydraulic coupling in the reactor and to generate the necessary reactivity coefficients to be used in SLOWKIN.[2, 3]

Conservation of mass and energy is applied to write the lumped parameter equations for the temperature within the regions of interest; these include the pool, the reactor upper and lower container water, the beryllium reflectors and the reactor core region. The reactor core region is subdivided into an arbitrary number of axial planes along which the radial heat transfer from an average fuel pin to the moderator/coolant will be considered and an axial temperature profile will be calculated in the fuel, in the fuel sheath and in the moderator.

Natural circulation of water through the core will be modeled with a correlation for the flow rate as a function of power–to–coolant in the reactor. This correlation is based on observations at steady-state in all SLOWPOKE–2 reactors. A sampled first-order filter will introduce a simple time-constant delay to represent the inertial effects. This approach is a major simplication which allows us to solve the transient temperature equations without solving the thermalhydraulics equations for natural circulation.

When fuel sheath temperature exceeds the saturation temperature, nucleate boiling will occur. In SLOWKIN. an appropriate correlation is used for the heat transfer coefficient to the coolant under subcooled nucleate boiling. Void formation is also predicted, and can become a dominant feedback mechanism.

The temperature and void models developpped for SLOWKIN will first be described. Some of the calculated transients for HEU and LEU reactors will then be presented in Section III.

II. The SLOWKIN Model

The point kinetics equations are solved in SLOWKIN for the amplitude $p(t)$ of the *neutron power*, which is arbitrarily normalized to one at the beginning of a transient:

$$p(0) = p_o = 1.0 \tag{1}$$

We have assumed that a fraction $f_{rc} \approx 95\%$ of the instantaneous fission power is deposited in the fuel, the remainder appearing in the moderator and in the reflector. Volumetric heat generation responsible for temperature changes in the reactor domain is proportionnal to the instantaneous *thermal power*, $P(t)$, which contains the instantaneous fission power as well as a delayed component $\Omega(t)$ associated with the decay power of the fission products ($\Omega_o = \kappa_{pf} \approx 7\%$ at steady state). We will calculate $P(t)$ as:

$$P(t) = P_o\left[(1 - \kappa_{pf})p(t) + \Omega(t)\right] \tag{2}$$

Transients are essentially driven by the dynamic reactivity, $\rho(t)$. In SLOWKIN, dynamic reactivity contains the following components:

$$\rho(t) = \rho_o + \rho_{cont}(t) + \rho_{temp}(t) + \rho_{void}(t) + \rho_{xenon}(t) \tag{3}$$

where ρ_o is the initial shutdown reactivity.

Simplified models are used for the control rod (ρ_{cont}) and for the xenon effect (ρ_{xenon}). We will now consider in detail the temperature and void components of the feedback model in SLOWKIN.

II.A. The SLOWKIN Temperature Model

Temperature feedback at time t will be function of the *average* temperature in various components of the reactor. Figure 1 illustrates the lump model used in SLOWKIN for the heat balance equations.

The unknowns are:

$T_1(t)$ The core average fuel temperature at time t;

$T_2(t)$ The average temperature of the water flowing through the core (coolant/moderator) at time t;

$T_3(t)$ The average temperature of the metallic berylium reflector at time t;

$T_4(t)$ The average temperature of the water in the downcomer located outside of the berylium reflector at time t.

$T_5(t)$ The average water temperature in the upper reactor container at time t;

$T_6(t)$ The average water temperature in the pool at time t;

The following assumptions are made to write the heat balance equations governing the temperature field in the reactor:

- Temperature is uniform within each control volume;
- 100% full power is defined for an absolute flux of 10^{12} nv at the flux detector site. Because of the different flux shapes, full power is different for HEU and LEU. We found with DRAGON/DONJON that $P_o^{(LEU)}/P_o^{(HEU)} = 1.0587$ for the same reading at the detector site.
- The core (fuel+moderator/coolant) is subdivided into M axial regions of equal volume. Heat is transfered laterally between the fuel and coolant volumes, and between the coolant and the berylium reflector. Thus, only radial thermal conduction is considered in the fuel pins: axial conduction is neglected;
- Volumetric heat generation in the fuel is *not uniform.* A fixed axial power profile is assumed in the fuel. This profile was obtained from the DONJON diffusion calculations and corresponds to the steady-state axial distribution of power (averaged over each plane). If $f_{\phi m}$ is the fraction of power produced at elevation m, then the *fuel linear heat rate* q_m is simply:

$$q_m(t) = \frac{f_{rc} f_{\phi m}}{N_c H_m} \cdot P(t) \tag{4}$$

  where N_c is the number of fuel pins in the core and $H_m = H/M$ is the length of the fuel section. The linear heat rate distribution at full power is illustrated in Figure 2. Because of the fewer fuel pins, we see that *the linear heat rate is significantly higher in LEU*;
- All water properties were evaluated for single phase liquid water at a constant pressure of 1.435 *bar*.

The SLOWKIN temperature equations are:

1. *Fuel* (T_1)

$$\frac{\kappa_{1,m}}{H_m} \cdot \frac{dT_{1,m}(t)}{dt} = q_m(t) - \frac{1}{R_{tot,m}} \left[T_{1,m}(t) - T_{2,m}(t)\right] \tag{5}$$

   where $T_{1,m}$ is the fuel temperature at elevation m in an average fuel pin, and $\kappa_{1,m}$ is the thermal capacity of the fuel. The thermal resistance is:

$$R_{tot,m} = R_{1,m} + \frac{1}{8\pi k_f \left(T_{1,m}\right)} \tag{6}$$

   with:

$$R_{1,m} = \frac{1}{2\pi r_f h_{gap,m}} + \frac{1}{2\pi k_g} \ln\left(\frac{r_s}{r_f}\right) + \frac{1}{2\pi r_s h_{cal,m}} \tag{7}$$

   where r_f and r_s are the inner and outer radius of the fuel sheath, respectively.

   Thermal resistance in the fuel is thus sensitive to the conductivity of the fuel (k_f), to the fuel/sheath gap heat transfer coefficient ($h_{gap,m}$), to the sheath thermal conductivity (k_g) and to the heat transfer coefficient to the coolant ($h_{cal,m}$).

The *gap resistance* is negligeable for HEU, while for LEU it is significant yet uncertain. Gap thickness is expected to vary from one pin to the other, so that values ranging from 5 to 20 $kW/m^2/°C$ are expected. To account for reduced gap resistance when the fuel expands with increasing power and comes in better contact with the fuel sheath, we have assumed the following relation in SLOWKIN for LEU fuel:

$$h_{gap,m}^{LEU}(t) = h_{gap,o} \cdot [1. + 10.\frac{q_m(t)}{q_o}] \tag{8}$$

where q_o is the average linear heat rate at nominal full power. A value of $h_{gap,o}$ =1.5 $kW/m^2/°C$ was arbitrarily chosen.

A constant thermal conductivity k_f is assumed for HEU fuel. For the ceramic UO_2 fuel (LEU), thermal conductivity is much smaller and is strongly dependent on temperature.[4] Consequently, a significant temperature gradient may arise in the fuel, and the above lump model can miscalculate the average fuel temperature. An option was programmed in SLOWKIN to obtain the radial temperature profile in the fuel pins by solving the heat conduction equation within the UO_2, using finite differences. We observed that the lump fuel model yields average fuel temperatures nearly identical to the profile temperature model, even for LEU fuel. The lump approximation is therefore considered valid even for fast transients in SLOWPOKE.

2. *Moderator/Coolant* (T_2)

$$\begin{aligned}\frac{dT_{2,m}(t)}{dt} &= \frac{(1-f_{rc})}{2 \cdot \kappa_{2,m}} f_{\phi m} P(t) + \frac{N_c H_m}{\kappa_{2,m} \cdot R_{tot,m}} [T_{1,m}(t) - T_{2,m}(t)] \\ &\quad - \frac{h_{Be} A_{1,m}}{\kappa_{2,m}} [T_{2,m}(t) - T_3(t)] + \frac{W\, C_p}{\kappa_{2,m}} [T_{2,m-1}(t) - T_{2,m}(t)] \quad , \end{aligned} \tag{9}$$

with the inlet coolant temperature $T_{2,0}(t) = T_4(t)$.

$\kappa_{2,m}$	The thermal capacity of the moderator/coolant at level m in the core;
$\frac{1-f_{rc}}{2}$	Fraction of fission energy deposited directly in region m of the moderator;
h_{Be}	Convection heat transfer coefficient between the moderator/coolant and the interior of the berylium reflector $[\frac{kW}{m^2 C}]$;
$A_{1,m}$	Heat transfer area between the moderator/coolant and the interior of the berylium reflector at level m ;
W	Natural circulation flow $[\frac{kg}{s}]$;

3. *Berylium Reflector* (T_3)

$$\kappa_3 \frac{dT_3(t)}{dt} = h_{Be} A_1 [T_2(t) - T_3(t)] - h_{Be} A_2 [T_3(t) - T_4(t)] + \frac{1-f_{rc}}{4} P(t) \quad , \tag{10}$$

4. *Water Reflector* (T_4)

$$\frac{dT_4(t)}{dt} = \frac{h_{B2}A_{B2}}{\kappa_4}[T_3(t) - T_4(t)] - \frac{h_{RP}A_{RP}}{\kappa_4}[T_4(t) - T_6(t)] + \frac{WC_p}{\kappa_4}[T_5(t) - T_4(t)] + \frac{1 - f_{rc}}{4\kappa_4}P(t) \quad , \tag{11}$$

5. *Upper Reactor Container Water* (T_5)

$$\frac{dT_5(t)}{dt} = \frac{W\,C_p}{\kappa_5}[T_{2,M}(t) - T_5(t)] - \frac{h_{CP}A_{CP}}{\kappa_5}[T_5(t) - T_6(t)] \quad , \tag{12}$$

where $T_{2,M}(t)$ is the core outlet coolant temperature, i.e. the temperature of the water flowing back into the upper container.

6. *Pool Water* (T_6)

$$\frac{dT_6(t)}{dt} = \frac{h_{RP}A_{RP}}{\kappa_6}[T_4(t) - T_6(t)] + \frac{h_{CP}A_{CP}}{\kappa_6}[T_5(t) - T_6(t)] \quad . \tag{13}$$

II.B. Temperature Feedback (ρ_{temp})

All temperature feedback effects are expressed relative to the same uniform reference temperature, $T_o = 20°C$. The temperature feedback will be function of T_1, T_2, T_3 and T_4. In regions 2 and 4, single phase water density variations with temperature (at a pressure of 1.4 bar) are included in the reactivity coefficients. The temperature feedback component in SLOWKIN will be written:

$$\begin{aligned} \rho_{temp}(t) &= a_1\Delta T_1(t) + a_{21}\Delta T_2(t) + a_{22}\Delta T_2(t)^2 + a_3\Delta T_3(t) \\ &\quad + a_4 \cdot [0.8\,\Delta T_4(t) + 0.2\,\Delta T_2(t)] \end{aligned} \tag{14}$$

where $\Delta T_k(t) = T_k(t) - T_o$.

The temperature reactivity coefficients used in this study are given in Table 1. The temperature reactivity effects have been studied in detail in transport and diffusion theory with DRAGON/DONJON.[2, 3] The following observations have been made:

- The reactivity coefficients were found to be additive in the range of interest;
- The most important *negative* effect is due to the moderator/coolant temperature changes. Accompanying liquid density variations account for the majority of the reactivity effect. The effect is strongly negative since the core region is undermoderated. Because of the larger moderator-to-fuel ratio in LEU, the spectrum is more thermalized and this reactivity component is smaller;

- The container water has a *positive* reactivity effect, because it lies in a fully thermalized neutron spectrum where reducing the water density reduces neutron absorption.

- The temperature of the water in the immediate vicinity of the core is not uniform. The water flowing down is cold (T_4) and determines the core inlet temperature ($T_{2,1} \approx T_4$). The water immediately above the core is warmer, being a mixture of the outlet coolant ($T_{2,M}$) and of the upper container water (T_5).

DONJON calculations have indicated that the fraction of the reflector reactivity coefficient associated with water *above* the core is 21 % for HEU and 34 % for LEU. This component is likely to vary more rapidly in a transient since it is related to the *outlet* coolant temperature. A larger value is obtained for LEU because the water volume is larger (absence of beryllium plates in the shim tray in the fresh core).

As a first approximation, we have assigned 20% of the positive reflector effect to the warm water *above* the core, at temperature T_2, and 80% to the downcommer water, at temperature T_4.

II.C. Heat Transfer and Subcooled Nucleate Boiling

An important aspect of the previous temperature model is the prediction of an appropriate circulation flow and the use of correct heat transfer coefficients.

II.C..1 Natural Circulation

If power in the reactor is maintained at a constant level, a fixed natural circulation flow will eventually be established. This *steady state flow* is the result of an equilibrium between the driving pressure difference (the buoyant driving force) and the pressure losses due to friction, acceleration and sudden changes in the geometry (viscous forces). For a fixed geometry (mostly the core flow orifice areas), there is therefore a fixed relationship between the natural circulation flow W and the power level P in the reactor. This translates into a fixed relationship between the power and the water temperature ΔT across the core. Since the inlet and outlet orifices are very similar, the measured ΔT as a function of power are very similar for all SLOWPOKE reactors. Using the experimental data reported in the safety report,[5] we can write:

$$\Delta T_{core} = exp(1.3074 + 0.59117 ln P) \tag{15}$$

For single phase flow, we have:

$$P = W \cdot C_p \Delta T \ , \tag{16}$$

We finally obtain the following correlation $W = f_W[P]$, shown in Fig. 3:

$$W = 0.00116P + 0.325\left(1. - e^{-0.05P}\right) \tag{17}$$

with W in [kg/s] and P in [kW].

Eq. (17) is valid at *steady state*. When power varies during a transient, the instantaneous flow rate takes a certain time to develop and is a function of the energy delivered to the coolant, rather than the instantaneous power in the fuel. During reactor transients in

all SLOWPOKE reactors, a delay of approximately 10-15 s following a prompt peak has been observed before the outlet temperature begins to rise.[5] To simulate this response in SLOWKIN, a sampled first order filter is introduced with a time constant τ_f, using the power-to-coolant $P_{cal}(t)$ in Eq. (17) instead of $P(t)$:

$$P_{cal}(t) = N_c H \sum_{m=1}^{M} \frac{[T_{1,m}^{(J)}(t) - T_{2,m}(t)]}{R_{1,m}} \tag{18}$$

The filtered response will be found as follows. Let x_n be the *unfiltered* response at time t_n, i.e. $x_n = f_W[P_{cal}(t_n)]$. Then the *filtered* response, $W(t_n) = y_n$, will be:

$$y_n = a \cdot y_{n-1} + b \cdot (x_n + x_{n-1})/2. \tag{19}$$

with

$$a = e^{-\Delta t/\tau_f} \quad \text{and} \quad b = 1. - a \tag{20}$$

and where $\Delta t = t_n - t_{n-1}$. The use of the correlation in Eq. (17) with the above first order filter is a major simplification: it avoids the complex transient thermalhydraulics equations required to satify the principle of conservation of momentum, but yet it should account for inertial effects. A value of $\tau_f = 10s$ was used for our simulations in SLOWKIN.

II.C..2 Heat Transfer Coefficient and ONB

An important term in the fuel temperature equations is the heat transfer coefficient h_{cal} between the fuel sheath and the bulk moderator/coolant. This coefficient will vary with local conditions of flow and temperature since coolant motion increases the rate of heat transfer.

A) Single-Phase Natural Convection

If the wall (sheath) temperature remains below the liquid saturation temperature (in our case, 112°C), the single-phase coefficient h_{cal} must be determined. When the thermal boundary layer thickness δ_T is much smaller than the cylinder diameter D, the curvature of the lateral surface does not play a role in the heat transfer and the Nusselt number can be calculated with vertical wall formulas. The Churchill and Chu correlation can be used to find the wall-averaged Nusselt number for the entire Rayleigh number range (laminar, transition, and turbulent):[6]

$$\overline{\mathrm{Nu}}_H = \left\{ 0.825 + \frac{0.387 \mathrm{Ra}_H^{1/6}}{\left[1 + (0.492/\mathrm{Pr})^{9/16}\right]^{8/27}} \right\}^2 \tag{21}$$

Thus, the single-phase heat transfer coefficient at axial position m is:

$$h_{SP,m} = \overline{\mathrm{Nu}}_H \cdot \frac{k_m}{H} \tag{22}$$

where the Nusselt number is function of the wall ΔT, i.e. the temperature difference between the fuel sheath and the bulk coolant: $\Delta T_{cal,m} = T_{S,m}(t) - T_{2,m}(t)$.

B) Subcooled Nucleate Pool Boiling

When the temperature of fuel sheath becomes slightly higher than the water saturation temperature, subcooled nucleate boiling takes place. With Onset of Nucleate Boiling (ONB), vapor forms locally at nucleation sites on the heating surface. Bubbles form in small cavities and grow at these sites. Since the coolant is subcooled, the vapor bubbles normally recondense in the liquid, giving rise to no net evaporation. If subcooling is high, the bubbles may not even detach from the wall. In any case, heat transfer is improved by the fluid motion near the wall.

As the fuel surface temperature is increased, vaporization will continue and more bubbles will form on the fuel surface at nucleation sites. Both the frequency of bubbles collapse or detachment and the number of nucleation sites will increase with the wall superheat, $\Delta T_{wall} = T_{wall} - T_{sat}$.

Therefore, once ONB is reached, heat transfer is dramatically improved. In this regime, the heat flux becomes a function of the wall superheat alone, independent of the subcooling (or the subcooled liquid temperature):

$$q''_{NB} = h_{NB} \cdot \Delta T_{wall} \quad . \tag{23}$$

We have used the Rohsenow correlation for the subcooled nucleate boiling regime in SLOWKIN.[7] This correlation can be written:

$$h_{NB} = \mu_l h_{fg} \left(\frac{g(\rho_l - \rho_v)}{\sigma} \right) \left[\frac{C_p}{\mathrm{Pr}_l^s \, C_{sf} \, h_{fg}} \right]^3 (T_S - T_{sat})^2 \, . \tag{24}$$

where T_S is the local sheath temperature. This correlation applies to clean surfaces and is insensitive to the shape and the orientation of the surface. The empirical value C_{sf} accounts for the particular combination of liquid and surface material, the exponent s, differentiates only between water and the other liquids, the subscripts l, v denote saturated liquid and saturated vapor. The symbol σ denotes the surface tension of the liquid in contact with its own vapor. Finally, h_{fg} is the latent heat of vaporization.

The heat flux from the fuel at position m can therefore be written:

$$\begin{aligned} q''_m(t) &= h_{cal,m} \cdot \Delta T_{cal,m} & (25) \\ &= h_{SP,m} \cdot (T_{S,m} - T_{2,m}) + h_{NB,m} \cdot (T_{S,m} - T_{sat}) & (26) \end{aligned}$$

The heat transfer coefficients obtained with the Rohsenow correlation are quite sensitive to the surface constant C_{sf}. Values given in the litterature range between 0.006 and 0.013 for stainless steel and water, depending on the quality of the surface (a more polished surface will bear fewer nucleation sites). For SLOWPOKE-2, we have arbitrarily assigned the value 0.006 for LEU, considering the zircalloy sheath in LEU to be equivalent to industrial stainless steel. For HEU, we have assumed a somewhat smaller value of 0.0045 for the aluminium sheath, because of its better conductivity and more porous surface. The resulting heat transfer coefficient is illustrated in Figure 4.

II.D. Void Fraction

DRAGON/DONJON simulations have shown that a very small amount of void can significantly reduce reactivity in SLOWPOKE-2. Typically, a 1% reduction in coolant density due to void can reduce dynamic reactivity by 4 mk. We first consider the prediction of the core average void fraction, $\alpha(t)$:

II.D..1 Wall Voidage

The subcooled nucleate boiling regime can be considered to be *partially developped* when bubbles remain attached to the wall (wall voidage). With increasing wall temperature, the bubbles grow beyond a critical size and detach from the wall. Once bubble detachment occurs, subcooled nucleate boiling is *fully developped* and more significant void fractions occur. An approximate model of the flow in the partially developped regime was proposed by Griffith. For highly subcooled flow boiling at moderate pressures, the void fraction is given by:[8]

$$\alpha_m = 3.73 \frac{q''_{NB,m}}{h_{SP}[T_{sat} - T_{2,m}]} \left(\frac{k_\ell}{h_{SP} D_h} \right) Pr_\ell \tag{27}$$

where D_h is the hydraulic diameter ($= 4S/P$). Because of the smaller number of pins, the hydraulic diameter is larger in LEU (4.2 cm vs 2.6 cm). Thus, the Griffith model recognizes that *in the partial nucleate boiling regime, void fraction is a function of the local conditions alone*: it increases with wall superheat, and it decreases with increasing subcooling.

II.D..2 Detached Voidage

Beyond the point of bubble detachment, the modeling efforts invariably require knowledge of how the bubble frequency, departure diameter and density of active nucleation sites vary with wall superheat. Despite years of research, these aspects of the boiling process are not well understood.[9]

A succesful alternative to mechanistic modelling is the profile-fit model of Zuber,[10] which was programmed in SLOWKIN. Let X_e^d be the (negative) thermodynamic quality at the point of bubble detachment. Then the *true quality* (always positive) is given by:

$$X = X_e - X_e^d \cdot e^{\left[\frac{X_e}{X_e^d} - 1\right]} \tag{28}$$

The void fraction is then obtained with the void-quality relation. Thus, the most important part of any effective subcooled boiling model is to be able to predict the void departure point. As water flows up the core, subcooling is gradually reduced, and could reach a critical subcooling at which bubble detachment occurs.

The following critical subcooling criteria have been proposed by Saha and Zuber for predicting the point of bubble detachment:[11]

- At low mass fluxes, bubble detachment depends only on local thermal conditions which determine the rates of vapour formation at the wall (proportional to the heat

flux) and the rate of condensation (proportional to the local subcooling). For *thermally controlled detatchment*, when the Peclet number $Pe = GD_H C_p/k < 70000$, the following criterion is used:

$$\Delta T_{sub} = 0.0022 \frac{q'' D_H}{k} \tag{29}$$

- At high mass fluxes ($Pe > 70000$), where mechanistic bubble detachment models are succesful, the process is *hydrodynamically controlled*. We have:

$$\Delta T_{sub} = 154 \frac{q''}{GC_p} \tag{30}$$

G is the mass flux. Pe is of the order of 2000-3000 in SLOWPOKE. Bubble detachment is clearly thermally controlled, and Eq. (29) generally applies.

II.D..3 Core Average Void Fraction and Slave Pin Calculations

In the above temperature model, the axial distribution of coolant temperature, $T_{2,m}(t)$, is obtained from the heat balance equation for an *average* fuel pin, since Eq. (5) uses the *average* linear rating at elevation m.

As we have seen above, initial void formation in the reactor is stricly dependent on local conditions. When a sheath temperature equal to saturation temperature is predicted in the average pin calculation, the lump model predicts no void formation, while in reality, a significant number of fuel pins are operating at a higher than average linear rating because the radial neutron flux shape is not uniform. The average pin calculation (lump) thus tends to underestimate the initial void formation in the core. The following approach is used in SLOWKIN to account for the nonuniform radial distribution of pin powers.

The distributions of pin power (relative to the average) were obtained from the 3D diffusion calculations in DONJON [3] These are assumed fixed during the transients. Separate *slave* calculations of fuel and fuel sheath temperatures are carried out for the different pin powers at each elevation, imposing the same coolant temperature $T_{2,m}(t)$ as a boundary condition at each elevation for every slave pin. The void profile is calculated for each group of fuel pins using the above correlations and a core volume average of the void fraction is then calculated, $\alpha(t)$.

II.D..4 Void Feedback (ρ_{void})

DONJON calculations indicate that void formation is neutronically more important in the top half of the core.[3] In SLOWKIN, a correction is introduced to account for the *axial* distribution of void, using an axial offset, f. An effective void coefficient at time t is obtained by interpolating between values in Table 2, according to:

$$\rho_{void}(t) = [b_1 \cdot f(t) + b_2 \cdot (1. - f(t))]\alpha(t) \times 100. \tag{31}$$

where the coefficients b_1 and b_2 are given in Table 6 (in $mk/\%$). The average void in the bottom half and in the top half are calculated (α_1 and α_2). The axial offset is simply $f = min\{1.0, \alpha_1/\alpha_2\}$.

III. SLOWKIN Results

Results of simulations for both HEU and LEU cores will now be presented. Three types of simulations were carried out, similar to the proposed commissionning tests. All calculations were carried out starting with xenon-free fuel, at a *reference temperature* of 20 °C for the pool and container water.

III.A. Core Heating Effects

For these simulations, the reactor is started up and brought rapidely to a given power level (neutron power). The reactivity change due to the temperature increase is compensated (and measured) by automatic control rod displacements. The values reported in Table 3 were calculated 10 minutes after startup from zero power (a period of approximately 5 minutes is required for the control rod position to stabilize). We noted that although LEU posesses a significant fuel temperature component, the core heating effects for LEU are approximately 35% *smaller than in HEU.* This is due to the significantly smaller moderator reactivity coefficient in LEU (see coefficient a_{21} in Table 1).

III.B. Long-Term Operation

During long-term operation at constant power, the slow temperature increase in the reactor container forces the gradual withdrawl of the control rod. This was simulated with SLOWKIN and results are shown in Figure 5, for constant operation at full power (10^{12} n/cm^2/s) for a period of 6 hours. Again, we note that the reactivity compensation is *smaller* in LEU, because the moderator coefficient is smaller. This implies that for a given excess reactivity margin, *the LEU core will permit full power operation for a significantly longer period.*

III.C. Self-limited Reactivity Transients

Self-limited reactivity transients occur when the control rod is removed from the reactor at low power. A *prompt peak* may first appear as an inflexion in the early part of the transient, and will gradually form a distinct peak as the reactivity insertion is increased. The prompt peak can become quite large, and depends on fast acting feedback mechanisms (fuel temperature, coolant heating, and incipient void) when natural circulation flow has not fully developped. Beyond the prompt peak, a *delayed peak* is generally observed, when the flow is fully develloped and the initial reactivity is completely compensated by the various feedback mechanisms described above.

Figures 6 and 7 show the reactivity transients calculated with SLOWKIN for HEU and LEU. We note that the prompt peak is not apparent for reactivity insertions below 4 mk. Table 4 describes the core behaviour at the delayed peak in LEU. Only core averaged quantities are given. We note that for all transients considered, margin to dryout is considerable (MCHFR). Tables 5 and 6 provide details of the reactivity compensation calculated in SLOWKIN for self-limited reactivity transients in HEU and LEU.

We note:

- For reactivity insertions of 0-3 mk, the delayed peak power is *higher* in LEU than in HEU, due to a smaller negative reactivity coefficient of the core water (moderator/coolant) and a larger positive coefficient for the water oustide the core (reflector);
- Fuel tempeature feedback plays a significant role in LEU, even for small perturbations. For example, at 2 mk, fuel temperature feedback represents 50 % of the negative component (see Table 6);
- SLOWKIN simulations indicate that *Onset of Nucleate Boiling (ONB) occurs in LEU for transients above 2.0 mk (for HEU, above 4.15 mk)*:
  - above 2 mk in LEU, void feedback plays an increasingly important role, with a value of approximately -1.0 mk at the delayed peak in the 4.3 mk transient (see Table 6);
  - beyond 4.3 mk, void feedback is likely to become the most important feedback mechanism in LEU. In HEU, void feedback becomes significant beyond 5 mk;
- The *core average* void fraction is quite small: for the 4.3 mk transient in LEU, the maximum core-average void fraction is less than 0.3 %. At the delayed peak, the core average *exit* void fraction is 0.42 %, with a maimum of 3.7 % in the hot pins (see Tables 7 and 8). There is no void in the cold pins.
- Bubble detachment (or so-called Onset of Significant Void) has not occured, because of the low flow and the very large subcooling (40 °C). Therefore, void formation in LEU is entirely due to *wall voidage* for transients up to 4.3 mk.

The delayed peak power predicted by SLOWKIN is compared with experimental data in Figure 8 (Tunney's Pasture for HEU cores and RMC for LEU cores). If the upcomming commissionning measurements at Ecole Polytechnique are similar to RMC, the trend suggested by Figure 8 is that SLOWKIN overpredicts the delayed peak beyond ONB. Considering the uncertainty in the wall voidage correlation (Eq. (27)), and our approximate treatment of the void coefficient (see section 2.2.3), the anticipated discrepancy in delayed peak power is not alarming.

IV. CONCLUSION

A simplified model was developed to simulate the transients occuring in the SLOWPOKE-2 reactor due to control rod movements. SLOWKIN was used to simulate transients in HEU and LEU. For LEU, these pre-simulations are subject to a number of uncertainties, relating mostly to:

- the reactivity effect of the warm water entering the upper container;
- the unknown gap resistance in the fuel;

- onset of nucleate boiling (ONB) which has a significant effect on the convection heat transfer to the moderator;
- the importance of void formation at high power, which rapidly becomes the limiting factor for the larger reactivity insertions;

Improvements are planned in the DRAGON/DONJON model, which may improve the reactivity coefficients. It is expected that future comparisons with the commissionning data will enable us to reduce some of the above uncertainties.

REFERENCES

[1] G. KENNEDY and G. MARLEAU, *"Refuelling the SLOWPOKE-2 Reactor at École Polytechnique: Procedure and Proposed Expperiments"*, 18th Annual Conference of the CNS, Toronto, Canada, June 1997.

[2] G. MARLEAU, S. NOCEIR, R. ROY and D. ROZON, *"DRAGON Modelling of the SLOWPOKE–2 Reactor at École Polytechnique"*, 18th Annual Conference of the CNS, Toronto, Canada, June 1997.

[3] S. NOCEIR, O. EL HAJJAJI, E. VARIN, R. ROY and D. ROZON, *"Diffusion Calculations for the SLOWPOKE–2 using DONJON"*,18th Annual Conference of the CNS, Toronto, Canada, June 1997.

[4] D.R. OLANDER, *" Fundamental Aspects of Nuclear Reactor Fuel Elements"*, ERDA Report TID-26711-P1, 1976.

[5] D.J. WINFIELD, *"Safety Analysis Report for the École Polytechnique SLOWPOKE–2 Reactor"*, AECL report RC-1598, October 1996.

[6] A. BÉJAN, *" Heat Transfer"*, John Wiley & Sons, Inc., 1993

[7] W.M ROHSENOW, *" A Method for Correlating Heat Transfer Data for Surface Boiling of Liquids"*, Trans.ASME, vol.84, p.969, 1962

[8] P. GRIFFITH, J.A. CLARK and W.M. ROHSENOW, *" Void Volumes in Subcooled Boiling Systems"*, Paper 58-HT-19, Nat. Heat Transfer Conf., Chicago, 1958

[9] Van P. CAREY, *" Liquid–Vapor Phase-Change Phenomena: An Introduction to the Thermophysics of Vaporization and Condensation Processes in Heat Transfer Equipment"*, Hemisphere Publishing Corp., 645 p. (1992)

[10] N. ZUBER, F.W. STAUB and G. BIJWAARD, *" Vapor Void Fractions in Subcooled Boiling and Saturated Boiling Systems"*, Proc.3rd Int. Heat Transfer Conf., Chicago, 1966

[11] P. SAHA and N. ZUBER, *" Point of Net Vapor Generation and Vapor Void Fraction in Subcooled Boiling"*, Proc.5th Int. Heat Transfer Conf., Vol. IV, 1974

Table 1: Reactivity Coefficients Calculated with DRAGON/DONJON

case	a_1	a_{21}	a_{22}	a_3	a_4
HEU (1987 plates/no rod)	0.000917	-0.134230	-0.0015817	0.008178	0.075356
LEU (no plates/no rod)	-0.010165	-0.047841	-0.0015449	0.002250	0.078580
LEU (no plates/rod 79 %)	-0.010165	-0.050980	-0.0015894	0.002254	0.077160

Table 2: Void Reactivity coefficients for SLOWPOKE–2 (in $mk/\%$ void)

core	b_1	b_2
HEU	-3.956	-4.997
LEU	-3.616	-4.656

Table 3: LEU Core Temperature Reactivity Effects (Constant Power, 10 minutes after startup)

P_{th}	*Fuel*		*Moderator*		*Be Reflector*		*Water Reflector*		*Control Rod*	**Measured**
(kW)	°C	*mk*	°C (out)	*mk*	°C	*mk*	°C (in)	*mk*	*mk*	**(RMC)**
1.962	29.68	-0.098	24.81	-0.143	20.68	0.002	20.04	0.046	0.240	0.24
4.865	37.56	-0.178	28.44	-0.264	21.27	0.003	20.10	0.082	0.372	0.44
9.729	47.22	-0.277	32.90	-0.432	22.10	0.005	20.22	0.129	0.595	0.68
19.46	62.04	-0.427	39.72	-0.731	23.48	0.008	20.49	0.207	0.957	1.17

Table 4: LEU-core Behaviour at Delayed Peak (core average)

Reactivity	*1 mk*	*2 mk*	*3 mk*	*4 mk*	*4.3 mk*
peak power (kW)	18.76	50.23	77.65	90.88	94.07
time (min)	37.2	14.8	7.9	5.0	4.6
T_{inlet} (°C)	21.18	21.17	20.86	20.63	20.61
T_{outlet} (°C)	40.09	55.09	64.82	69.80	68.89
$T_{moderator}$ (°C)	31.74	40.04	45.30	47.45	47.93
T_{fuel} (°C)	61.73	96.06	119.59	129.44	131.58
T_{sheath} (°C)	57.85	88.41	108.47	116.40	118.19
void (%)	0.0	0.0	0.043	0.181	0.233
flow (kg/s)	0.228	0.342	0.408	0.435	0.442
MCHFR	34.86	12.04	7.51	6.27	6.03

Table 5: Reactivity Compensation (mk) at the Delayed Peak in HEU

Insertion (*mk*)	*Peak Power* (*kW*)	ρ_{fuel} (*mk*)	ρ_{mod} (*mk*)	ρ_{refl} (*mk*)	ρ_{void} (*mk*)
1.0 mk	10.12	0.020	-1.154	0.167	0.0
2.0 mk	28.78	0.038	-2.274	0.289	0.0
3.0 mk	51.56	0.054	-3.384	0.391	0.0
4.0 mk	76.52	0.068	-4.476	0.481	-0.002
5.0 mk	95.68	0.078	-5.191	0.515	-0.334
6.0 mk	107.26	0.082	-5.504	0.526	-1.011

Table 6: Reactivity Compensation (mk) at the Delayed Peak in LEU

Insertion (*mk*)	*Peak Power* (*kW*)	ρ_{fuel} (*mk*)	ρ_{mod} (*mk*)	ρ_{refl} (*mk*)	ρ_{void} (*mk*)	**Measured (RMC)**
1.0 mk	18.76	-0.424	-0.774	0.269	0.0	18 kW
2.0 mk	50.23	-0.773	-1.579	0.409	0.0	40 kW
3.0 mk	77.65	-1.012	-2.199	0.466	-0.189	55 kW
4.0 mk	90.88	-1.112	-2.478	0.483	-0.803	77 kW
4.3 mk	94.07	-1.134	-2.545	0.491	-1.036	N/A

Table 7: Axial Temperature Distribution in LEU for the 4.3 mk Insertion at the Time of Maximum Void (6.4 min)

plane	Tmod (°C)	Tsheath (°C)	Tfuel (°C)	void (%)	heat flux (kW/m2)	CHFR
15	70.304	126.328	138.025	0.418	101.542	6.582
14	67.603	123.059	134.128	0.184	96.018	7.160
13	65.048	123.214	134.828	0.177	101.700	6.938
12	62.333	124.157	136.610	0.206	110.301	6.571
11	59.378	124.849	138.121	0.222	118.723	6.281
10	56.186	125.001	138.957	0.212	125.815	6.107
9	52.794	124.518	138.973	0.176	131.062	6.045
8	49.252	123.335	138.071	0.123	134.178	6.092
7	45.618	121.396	136.180	0.066	135.093	6.241
6	41.950	118.607	133.191	0.023	133.888	6.491
5	38.309	115.048	129.245	0.002	130.799	6.841
4	34.744	110.862	124.519	0.000	126.240	7.288
3	31.297	106.614	119.707	0.000	121.232	7.791
2	27.979	103.378	116.150	0.000	118.602	8.162
1	24.726	104.022	117.439	0.000	125.531	7.894

Table 8: Void Distribution in % for the 4.3 mk Insertion in LEU (Slave Calculation)

slave group	1	2	3	4	5	6	7	8	9	10
no pins	30	46	38	34	24	10	8	2	4	2
power/avg.	0.825	0.894	0.965	1.037	1.108	1.179	1.251	1.322	1.393	1.465
plane 15	0.022	0.097	0.257	0.510	0.865	1.302	1.824	2.407	3.038	3.757
14	0.001	0.021	0.092	0.237	0.463	0.776	1.168	1.635	2.153	2.726
13	0.000	0.018	0.085	0.227	0.453	0.770	1.161	1.626	2.148	2.708
12	0.001	0.022	0.100	0.260	0.510	0.848	1.270	1.756	2.297	2.889
11	0.001	0.024	0.108	0.278	0.541	0.896	1.333	1.835	2.382	3.013
10	0.000	0.020	0.099	0.265	0.528	0.876	1.312	1.809	2.359	2.985
9	0.000	0.011	0.074	0.221	0.463	0.791	1.208	1.686	2.218	2.821
8	0.000	0.003	0.044	0.157	0.360	0.654	1.033	1.475	1.972	2.540
7	0.000	0.000	0.016	0.087	0.239	0.478	0.803	1.196	1.639	2.146
6	0.000	0.000	0.002	0.033	0.126	0.301	0.557	0.884	1.270	1.711
5	0.000	0.000	0.000	0.005	0.045	0.145	0.324	0.574	0.887	1.252
4	0.000	0.000	0.000	0.000	0.006	0.048	0.146	0.314	0.547	0.838
3	0.000	0.000	0.000	0.000	0.000	0.007	0.047	0.139	0.293	0.508
2	0.000	0.000	0.000	0.000	0.000	0.000	0.013	0.062	0.164	0.325
1	0.000	0.000	0.000	0.000	0.000	0.001	0.021	0.083	0.204	0.384

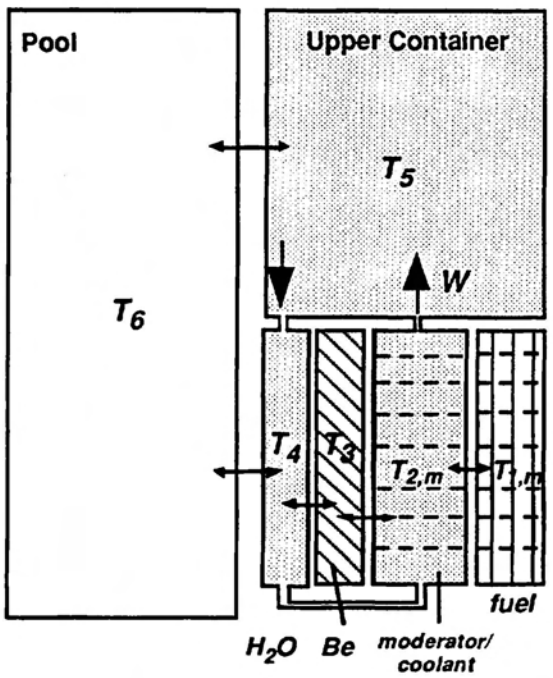

Figure 1: Temperature Model for SLOWPOKE–2

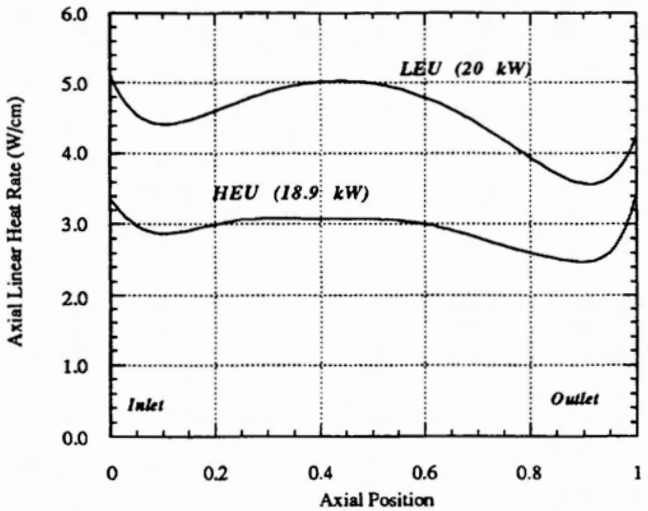

Figure 2: Axial Linear Heat Rate Distribution for SLOWPOKE–2 (full power)

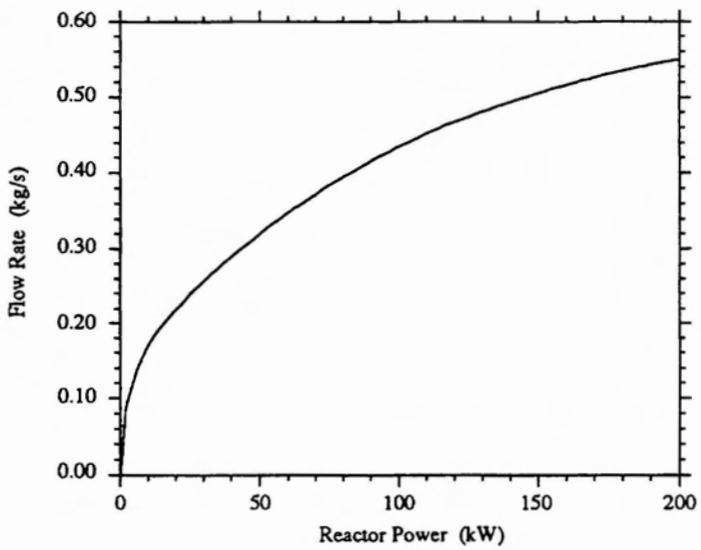

Figure 3: Natural Circulation Flow Rate in SLOWPOKE at Steady State

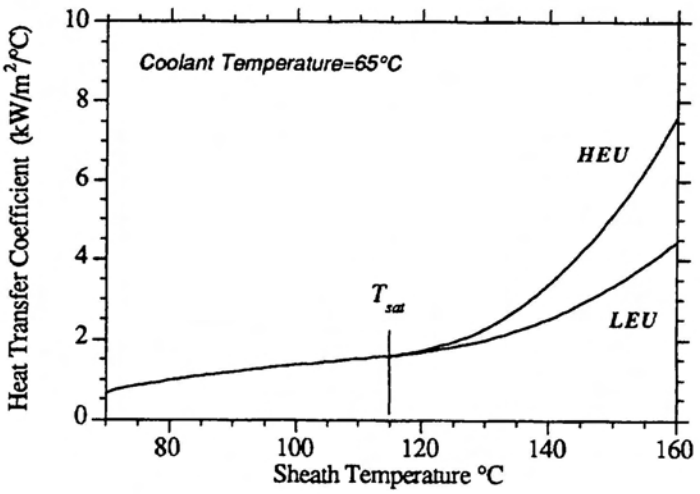

Figure 4: Heat Transfer Coefficient for SLOWPOKE–2

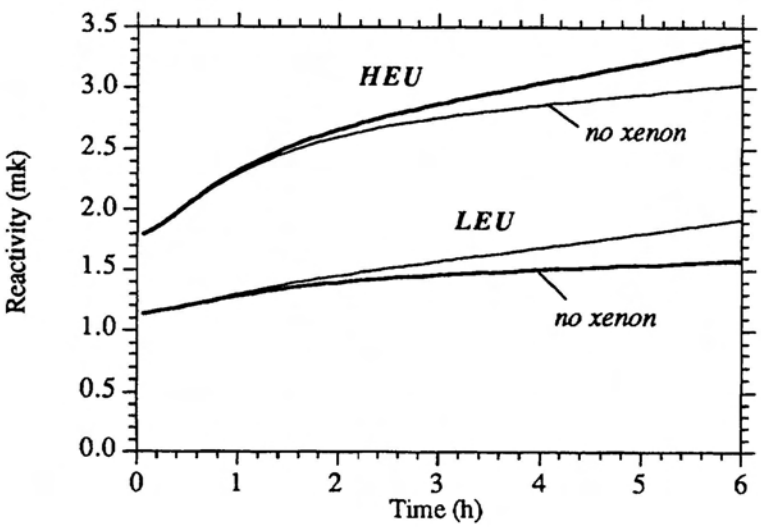

Figure 5: Reactivity Compensation at 100% Power

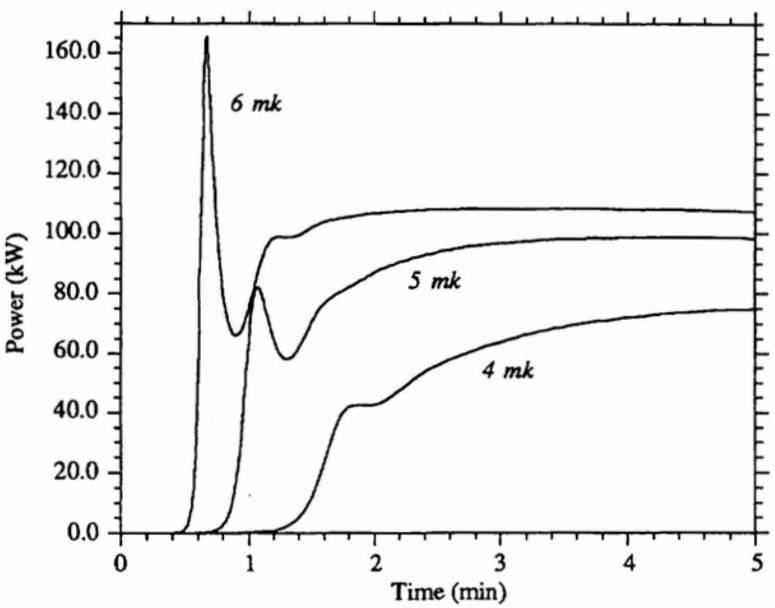

Figure 6: Self-limited Reactivity Transient in HEU (4-6 mk)

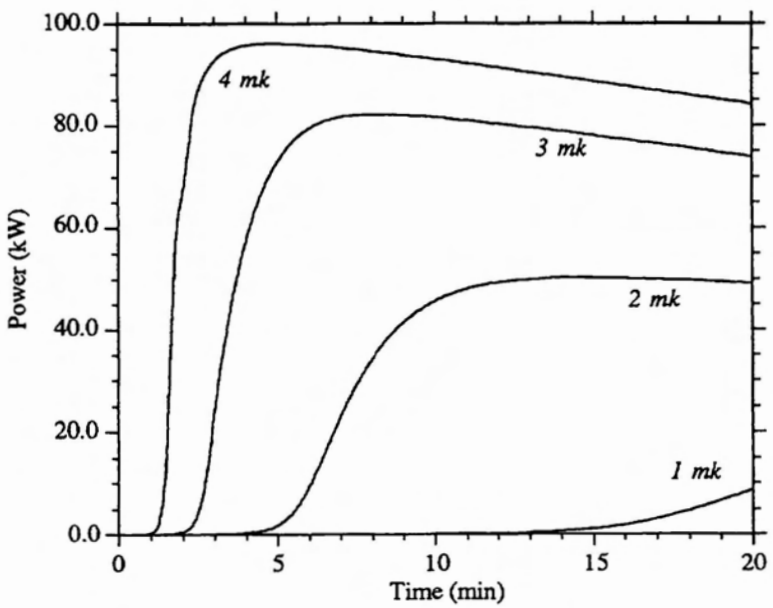

Figure 7: Self-limited Reactivity Transient in LEU (1-4 mk)

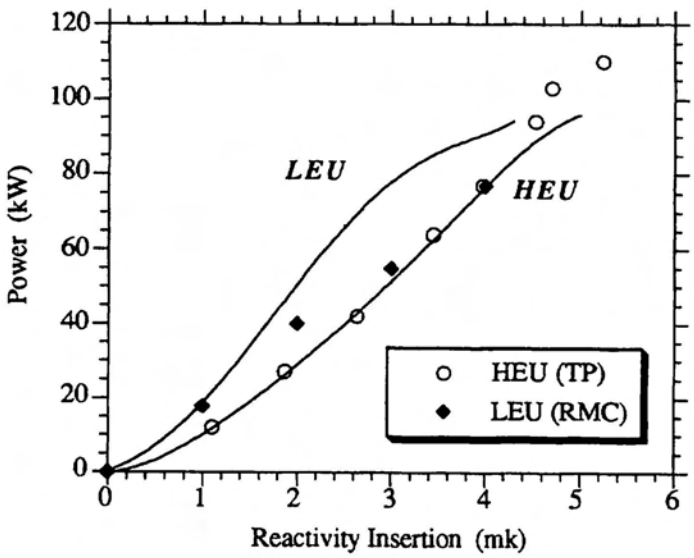

Figure 8: Delayed Peak Power in SLOWPOKE